High-resolution studies of extreme-ultraviolet emission from CO by electron impact

Marco Ciocca, Isik Kanik, and Joseph M. Ajello
Jet Propulsion Laboratory, California Institute of Technology, Pasadena, California 91009
(Received 9 May 1996; revised manuscript received 15 January 1997)

We report a high-resolution study (0.0036 nm full width at half maximum) of electron-impact-induced emission spectra of CO at 30-, 75-, and 100-eV electron-impact energies. The spectral features were acquired in optically thin conditions. At the specified resolution, attainable with our 3-m vacuum ultraviolet spectrometer, we observe rotationally resolved emission bands of CO in the extreme ultraviolet, from the vibronic states $B\ ^1\Sigma^+(0)$, $C\ ^1\Sigma^+(0)$, and $E\ ^1\Pi(0)$, to the ground state $X\ ^1\Sigma^+(0)$. A simple model of these bands, based on the Hönl-London factors and the rotational constants, is constructed and is shown to be in good agreement with the observed spectra. The predissociation yield for the $E\ ^1\Pi$ electronic state has been determined, showing that the E state has the largest predissociation cross section of CO for all singlet-state Rydberg series members. The excitation function of the $[E\ ^1\Pi(0)\rightarrow X\ ^1\Sigma^+(0)]$ transition, in the 0–800-eV impact energy range, is measured, permitting determination of the oscillator strength by using a modified Born approximation analytical fit. [S1050-2947(97)08004-9]

PACS number(s): 34.80.Gs

INTRODUCTION

As the most abundant interstellar molecule after H_2 [1], CO plays a very important role in the photochemistry of the interstellar medium (ISM) [2]. While H_2, in most cases, cannot be detected directly, CO is readily observed by radioastronomy and therefore has been utilized as a tracer molecule [3] for molecular hydrogen. The abundance ratio of CO to H_2 is difficult to determine from observations of the ISM, but can be obtained through theoretical models [4]. These models involve chemical reactions in which photodissociation by vacuum ultraviolet radiation (vuv) is the main destruction mechanism for CO [1], particularly in the range between 91.2 nm, which is the edge of the absorption continuum of atomic hydrogen, and 111.8 nm, which is the dissociation limit of CO into ground-state atoms. The rate of photodissociation of CO by vuv is one of the major uncertainties in these models. In view of these uncertainties and the importance of carbon monoxide as a tracer molecule, a large number of experimental studies has been performed. These studies were aimed at finding coincidences between molecular hydrogen emission lines and CO absorption lines, and at establishing the photodissociation rate in CO. A variety of techniques were used, including classical spectrographs [5,6], synchrotron radiation [7–10], and laser methods [11–13]. A review of molecular parameters (wavelengths and oscillator strengths) of CO with comparison with uv data has been published recently [14]. It clearly points out the large variation (a factor of 2) in the oscillator strengths of the B-X, C-X, and E-X transitions of the strongest Rydberg states (B,C,E) of CO. This factor remains a major obstacle in modeling the ISM. These states have prominent (0,0) vibronic bands in the extreme ultraviolet (euv). For this reason, we have carried out a high-resolution euv measurement of single-scattering excitation of the rotational line structure by electron impact. We have recently reported [15] the oscillator strengths of the $B\ ^1\Sigma^+(0)\rightarrow X\ ^1\Sigma^+(0)$ and $C\ ^1\Sigma^+(0)\rightarrow X\ ^1\Sigma^+(0)$ transitions and, in this paper, we report the oscillator strength of the $[E\ ^1\Pi(0)\rightarrow X\ ^1\Sigma^+(0)]$ transition.

Of the dozen or more bound states in the singlet state manifold structure of CO, the E-state photoabsorption cross section dominates all discrete dissociation channels [7]. Photodissociation can occur in two ways: either by continuum absorption into repulsive electronic states or via line absorption into predissociating states [16]. Experimental evidence [5,10,17] indicates that the latter mechanism is the most important for CO. In particular, line absorption into $ns\sigma$, $np\sigma\ ^1\Sigma^+$, and $np\pi\ ^1\Pi$ Rydberg series can be used to explain the absorption spectrum. Although the $3p\sigma C\ ^1\Sigma^+(0)$ vibronic state has the largest absorption cross section in the euv [7], there is no evidence of either predissociation [7] or accidental predissociation [13]. All Rydberg states for all Rydberg series above the $E(0)$ vibronic level are 100% predissociated, as shown schematically in Fig. 1. The $E(0)$ level is particularly interesting since it has the second largest absorption cross section in the euv [7] but is subject to only weak predissociation, as judged by the observed $E(0,0)$ band [15].

A comprehensive set of works on predissociation has been carried out recently using euv laser spectroscopy [12,13,18]. Predissociation reduces the lifetime of the excited state and may be detected as line broadening, which can affect the whole rotational manifold via direct coupling to the continuum or can affect a few rotational levels via accidental predissociation [12]. Laser spectroscopy studies for cases of strong predissociation have shown that the predissociation rates of CO can depend not only on which particular vibronic states are excited, but also on the rotational substates and even on the Λ-doublet component of $^1\Pi$ states [18]. Because of the competition between radiative and dissociative channels, however, the fluorescence from predissociating states is reduced. Therefore, emission studies are a more sensitive probe of predissociation. As an example, in the medium resolution study of Ajello *et al.* [19], predissociation rates for the vibrational levels of the $c_4'\ ^1\Sigma_u^+$ state of N_2, the isoelectronic equivalent of CO, were so obtained, by

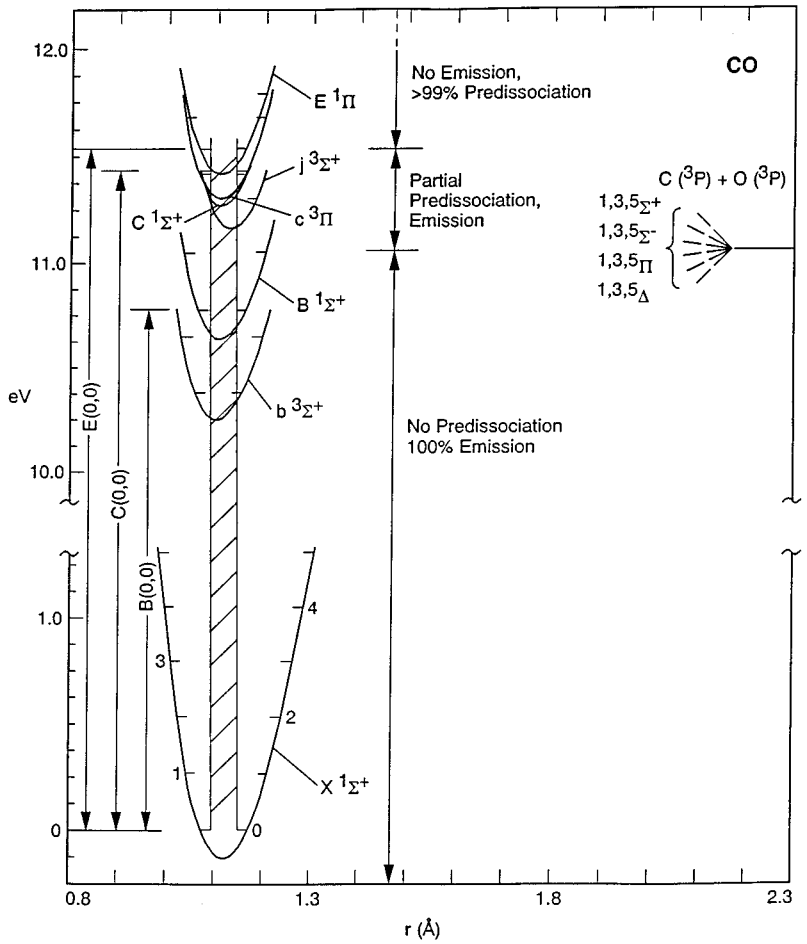

FIG. 1. Partial potential-energy curve diagram, emphasizing the 9.5–12.5-eV region. Shown are the potential-energy curves of the levels of CO studied in this work and the Franck-Condon region.

comparing emission to excitation cross sections.

Our group at the Jet Propulsion Laboratory has also previously published both low-resolution [20] and medium-resolution [15] studies of the electron-impact-induced emission spectra of CO in the range 91–116 nm, showing transitions from the states $B\ ^1\Sigma^+(0)$, $C\ ^1\Sigma^+(0)$, and $E\ ^1\Pi(0)$, to the ground state $X\ ^1\Sigma^+(0)$. The internuclear distance for the minima in the potential curves of the Rydberg and valence states of CO overlies exactly at the minimum of the ground state, as shown in Fig. 1, resulting in intense (0,0) bands. In our earlier study [15], we reported the emission cross sections, together with a determination of the excitation function for the $B(0,0)$ and $C(0,0)$ transitions. Oscillator strengths for these transitions were also reported [15]. At the spectral resolution under which those spectra were obtained [full width at half maximum (FWHM) of 0.025 nm], it was not possible to observe the rotational line structure of the transitions in question. In our present search for the rotational sublevel dependence of predissociation, we show the CO emission spectra for transition from the $B(0)$, $C(0)$, and $E(0)$ states to the ground state. With a FWHM of 0.0036 nm, we can resolve the rotational structure of the $E(0,0)$, $C(0,0)$, and $B(0,0)$ transitions. The main goal is to model the E-state rotational line intensities to (1) determine the suitability of the Hönl-London factors for their description and (2) distinguish between Π^+ and Π^- predissociation rates. In addition, the excitation function for the $E\ ^1\Pi(0) \rightarrow X\ ^1\Sigma^+(0)$ band is measured. By fitting the shape of the excitation function with an analytical expression based on the modified Born approximation [21,22], the oscillator strength is also determined.

In the remainder of this paper, we describe the experimental apparatus, the high-resolution measurements of the (0,0) resonance transitions of the B, C, E states, the spectroscopic model, and finally the measurement of the $E(0,0)$ excitation function and modified Born approximation analysis.

EXPERIMENTAL APPARATUS

The experimental apparatus has been described in detail elsewhere [23]. In brief, a high-resolution 3.0-m spectrometer system was used. It consists of an electron-impact collision chamber in tandem with a uv spectrometer. uv emission spectra of CO were measured by crossing a magnetically collimated beam of electrons with a beam of CO gas. A Faraday cup, designed to minimize detection of backscattered and secondary electrons, was used to monitor the electron current.

To acquire emission spectra, the beam of CO, formed by a capillary array, was crossed by an electron beam at 90°. The impact energy of the electron beam was kept fixed and emitted photons, corresponding to radiative decay from the collisionally excited states of CO, were dispersed by the uv spectrometer and then detected by a channeltron detector. Scanning of the wavelength was achieved by means of an indexed stepper motor. Occasionally, uneven motion (missed step) in the stepper motor could cause an uncertainty in the wavelength increments of about 0.002 Å (about half of the smallest increment possible) over the entire spectrum.

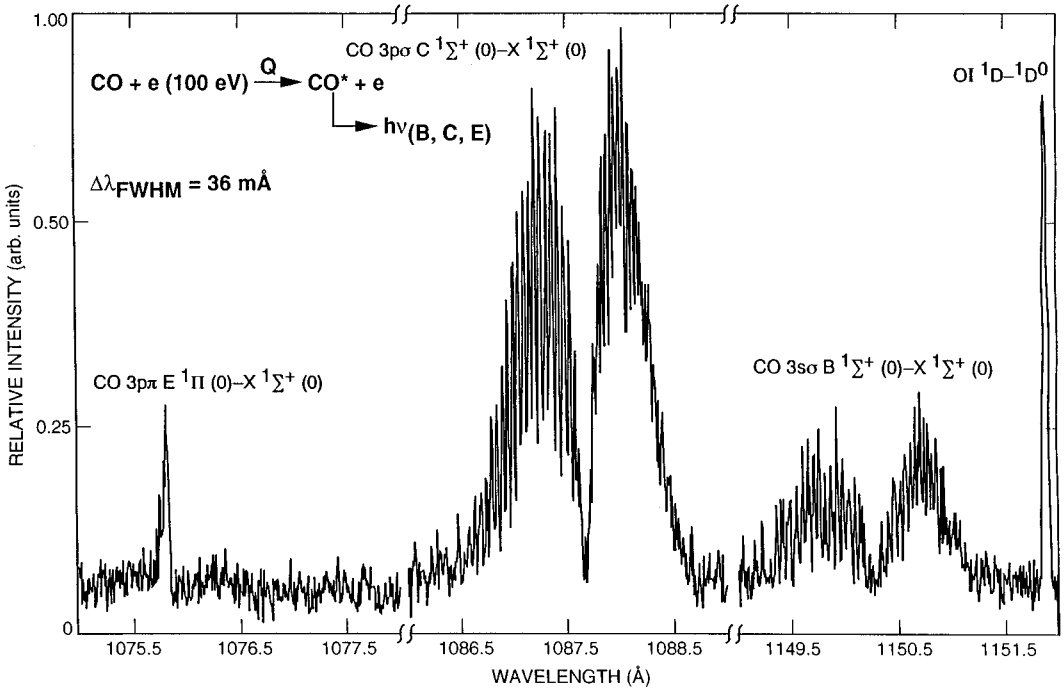

FIG. 2. High-resolution (0.036-Å FWHM with 8-mÅ step size) electron-impact-induced fluorescence spectrum of CO at 100 eV. The spectrum was obtained at a background pressure of 1.0×10^{-5} Torr. P and R branches are resolved for the $C(0,0)$ and $B(0,0)$ transitions, but only the Q branch appears for the $E(0,0)$.

A resolving power of $\lambda/\Delta\lambda\cong30\,000$ was achieved by operating the spectrometer in second order, with both entrance and exit slits equally set at 20 μm. The slit function at this setting was triangular, with a resolution of 0.036 ± 0.002 Å FWHM. The emission spectra were obtained at various incident electron energies. In particular, spectra were obtained at 30 eV for the $B(0,0)$ transition, 75 eV for the $E(0,0)$, and 100 eV for all the bands of interest.

An excitation function measurement for the $E(0)$ state was carried out at a specific wavelength (1076.1 Å) by measuring the relative intensity of the emitted radiation as a function of the electron beam energy. In this case a uniform static sample of CO was admitted to the chamber, forming a cylindrical line source in the collision region, thereby eliminating problems associated with a possible variation in size of the electron beam with changing energy.

All transitions observed in this study are toward the ground state of CO, $X\ ^1\Sigma^+(0)$ and, therefore, to ensure optically thin spectra, care must be taken in choosing the operating pressure. If the optical depth at line center of the strongest rotational lines is less than 0.1, self-absorption effects can be neglected. Below this pressure the measured cross section will be independent of pressure. The procedure used to determine the maximum background pressure that can be used while maintaining optically thin conditions has been presented in detail elsewhere [15]. The photon path length from the interaction region to the entrance slit of the spectrometer was 11.0 cm and the temperature of the gas was estimated to be approximately 330 K, due to heating from the coils that generate a magnetic field to collimate the e beam and the hot filament in the electron gun. This estimate was later confirmed by our model spectra (see experimental results below). Optically thin conditions were achieved by maintaining a background gas pressure in the collision chamber of less than 4.0×10^{-5} Torr for the E state and less than 1.0×10^{-5} Torr for the B and C states.

EXPERIMENTAL RESULTS

The measurements described here involve highly excited states of CO. A schematic potential energy diagram (in which the states studied are indicated) is presented in Fig. 1. The shaded area indicates the Franck-Condon region. The high-resolution, electron-impact emission spectra of $B\ ^1\Sigma^+(0)\rightarrow X\ ^1\Sigma^+(0)$, $C\ ^1\Sigma^+(0)\rightarrow X\ ^1\Sigma^+(0)$ and $E\ ^1\Pi(0)\rightarrow X\ ^1\Sigma^+(0)$ transitions are in the 1070–1160-Å region, and are shown in Figs. 2, 3, 4, and 5. Figure 2 gives an overview of all the features of the euv spectrum of CO studied in this work, with their identifications. The spectra were obtained at 100-eV electron-impact energy, with a background gas pressure of 1.0×10^{-5} Torr, in order to avoid effects of self-absorption, especially for the $C\ ^1\Sigma^+\rightarrow X\ ^1\Sigma^+(0)$ band, which has the largest oscillator strength of the three bands studied [15].

The spectral region from 1075.4 to 1077.5 Å contains the direct transition from the $E\ ^1\Pi(v'=0)$ to the ground state, while the region from 1086.5 to 1088.5 Å shows the rotationally resolved transitions from the $C\ ^1\Sigma^+(0)$ again to the ground state of CO. The $C\ ^1\Sigma^+$ state has been the subject of numerous spectroscopic investigations (see, for example, Tilford and Vanderslice [24]). More recently, Eidelsberg *et al.* [5,6] performed an absorption study of this state in the euv, while an extensive study employing laser spectroscopic techniques has been reported by Ubachs *et al.* [13]. In the 1149.5–1151.5-Å spectral region, we observe the transition from the $B\ ^1\Pi(0)$ excited state of CO to the ground state and an atomic component (OI $^1D-{}^1D^0$) at 1152.15 Å [25]. The $B\ ^1\Pi(v')\rightarrow X\ ^1\Sigma^+(v'')$ vibronic bands have been studied in

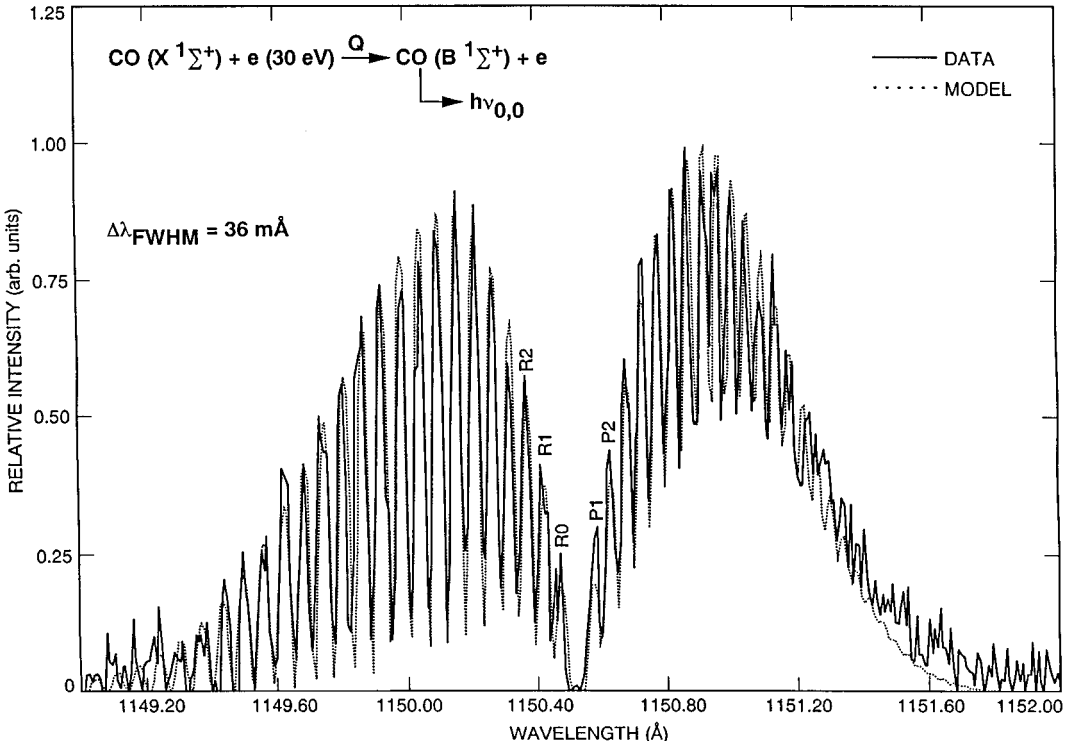

FIG. 3. Comparison between data and model for the $B\ ^1\Sigma^+(0)\rightarrow X\ ^1\Sigma^+(0)$ transition. The rotational line intensities in the model, based on the Hönl-London factors and the rotational constants of Ubachs *et al.* [18], have been convoluted with a triangular response function (0.036-Å FWHM). Indicated are the first few rotational lines of each branch.

detail by Eidelsberg *et al.* [26], both in absorption and in emission. They obtained the emission spectrum by means of a discharge lamp, with a CO pressure of few millitorr. No emission was observed from the $v=2$ level, indicating predissociation. Furthermore, a weakening of the emission lines in the $v=1$ and $v=0$ levels was also observed. This effect occurred above $J'=17$ and 37, respectively, thus indicating the onset of predissociation.

Kanik *et al.* [15] reported that the $B\ ^1\Sigma^+(0)\rightarrow X\ ^1\Sigma^+(0)$ band exhibits an anomalous behavior, showing a sharp peak in the excitation function at very low electron impact. For this reason, we obtained a spectrum of the $B\ ^1\Sigma^+(0,0)$ transition at an electron-impact energy of 30 eV, which corresponds to the maximum of the emission cross section for this state [15]. The results are presented in Fig. 3. The data shown were taken with a step size of 8 mÅ, and a resolution where the individual J levels up to $J=19$ for the R branch are clearly resolved. In this figure we also compare the measured spectrum with the output of our model, which will be described in detail below.

The model, based on the Hönl-London factors, makes use of the rotational constants of Ubachs *et al.* [18] for this state, and of Huber and Herzberg [27] for the ground state. The model generates emission intensities and wavelengths for the rovibronic transitions from the excited state to the ground state. No effects of perturbation by nearby states are included.

One of the parameters of the model is the temperature of the gas sample. It was found that the best agreement between data and model was achieved by adopting a temperature value of 330 K, which confirmed our estimate of the gas temperature in the interaction region. By convoluting the model intensities with the triangular slit function of the spectrometer, we obtain a synthetic spectrum that can then be compared with the measured spectrum. The model output and the data are both normalized to unity, to facilitate comparison. We obtain good overall agreement, as shown in Fig. 3. The triplet-state admixture [15] does not seem to affect the singlet character of the state to any great extent. Small discrepancies in intensity are observed between the model and the data. These cannot be attributed to a small amount of predissociation, since we do not observe the high rotational level ($J=37$) after which predissociation becomes important [26]. The small discrepancies are partly due to signal fluctuation, probably caused by the occasional irregularities in the wavelength increments, signal statistics, and possibly by a small amount of perturbation by nearby triplet states (see Fig. 1).

In Fig. 4 we present a spectrum of the $C\ ^1\Sigma^+(0)\rightarrow X\ ^1\Sigma^+(0)$ transition. The vibronic energies of the $C\ ^1\Sigma^+(v'=0,1)$ levels lie above the dissociation limit, 11.09 eV, so that they may either predissociate or decay via fluorescence (see Fig. 1). Letzelter *et al.* [7] reported that the predissociation yield of the $C(0)$ level is, at the most, 10%, while the $C(1)$ is almost entirely predissociated. The $C\ ^1\Sigma^+(0)\rightarrow X\ ^1\Sigma^+(0)$ transition, shown in Fig. 4, contains approximately 98% of the euv emission between the $C\ ^1\Sigma^+$ state and the ground state ([20] and references therein). Here again our model (which does not contain any predissociation terms) is in fairly good agreement with the observed spectrum. Small discrepancies are present. As stated in the case of the B state, these discrepancies are probably due to the occasional missed step in the wavelength increments, signal

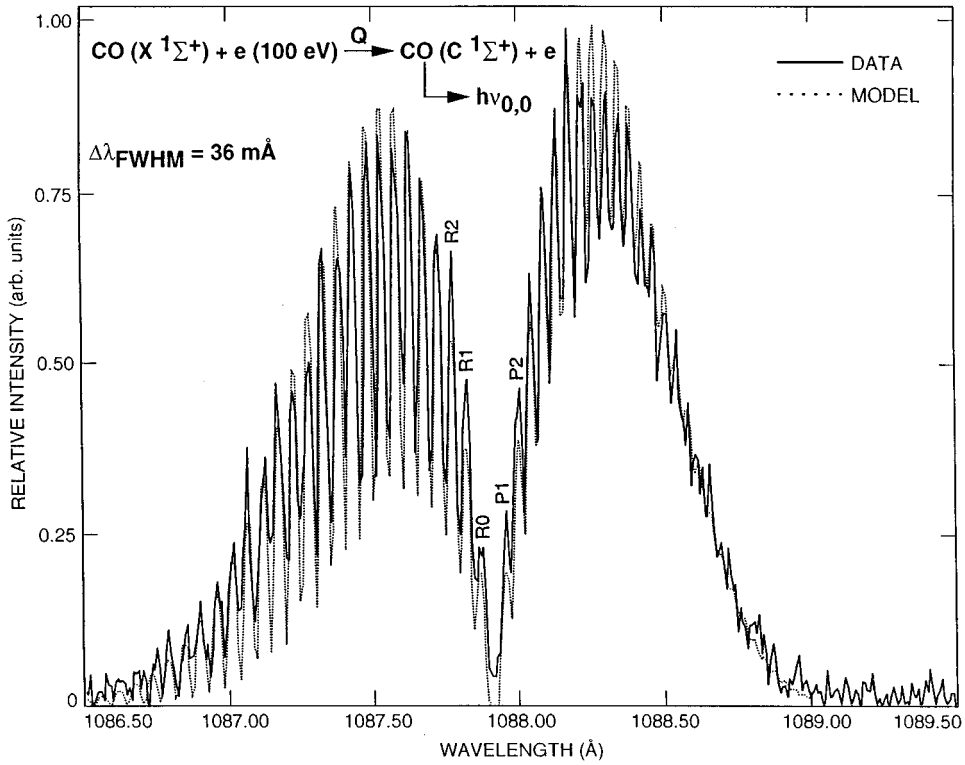

FIG. 4. Comparison between data and model for the $C\ ^1\Sigma^+(0) \rightarrow X\ ^1\Sigma^+(0)$ transition. The rotational line intensities in the model, based on the Hönl-London factors and the rotational constants of Ubachs *et al.* [18], have been convoluted with a triangular response function (0.036-Å FWHM). Indicated are the first few rotational lines of each branch.

statistics, and by perturbation from nearby triplet states (see Fig. 1).

In Fig. 5 we show the spectrum of the $E\ ^1\Pi(0) \rightarrow X\ ^1\Sigma^+(0)$ transition, which is compared with the model output (this time a predissociation term was included in the model). The model makes use of the rotational constants of Eidelsberg *et al.* [5], and of Huber and Herzberg [27] for the ground state. This transition was first observed by Hopfield and Birge [28] in emission and later analyzed, at higher resolution, by Tilford *et al.* [29]. This led to the con-

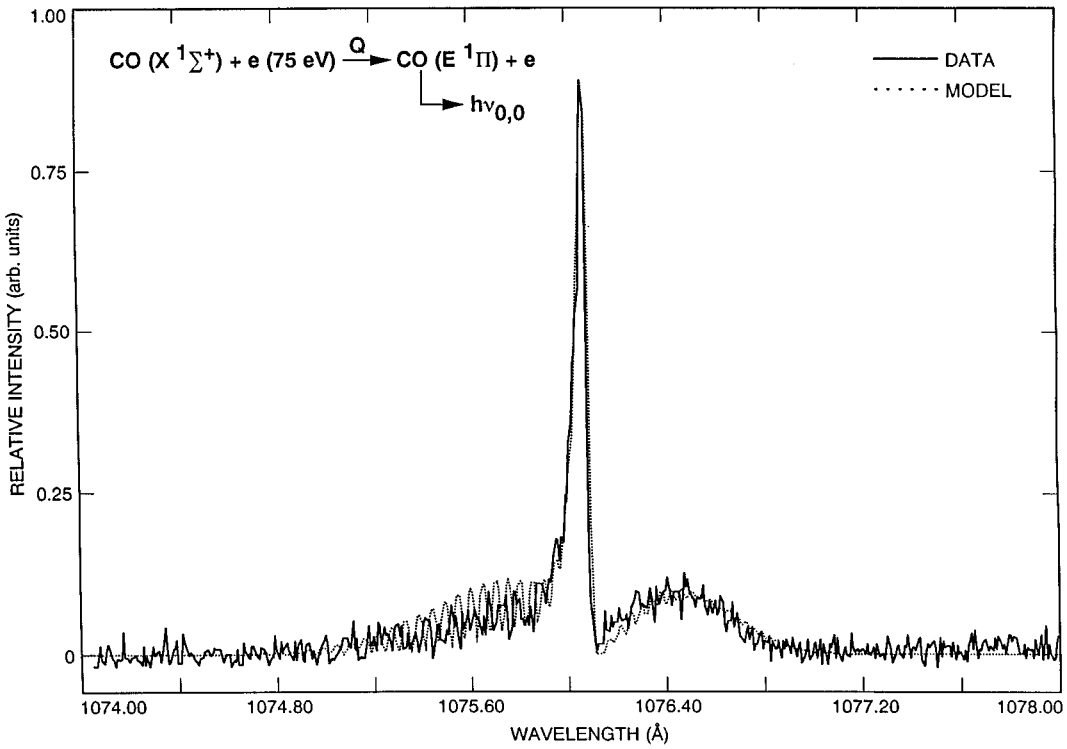

FIG. 5. Comparison between data and model for the $E\ ^1\Pi(0) \rightarrow X\ ^1\Sigma^+(0)$ transition. The rotational line intensities in the model, based on the Hönl-London factors and the rotational constants of Eidelsberg *et al.* [5], and with a ratio of 0.63 between the Q branch (Π^- state) the P and R branch (Π^+ state) predissociation yields, have been convoluted with a triangular response function (0.036-Å FWHM).

clusion that the level $E\ ^1\Pi(0)$ was not predissociated. Lee and Guest [17], however, found very weak fluorescence from this state and Letzelter *et al.* [7] were able to determine that the $E(0)$, although still fairly intense in emission spectra, was indeed predissociated. This was determined with a measurement of the fluorescence yield after excitation by synchrotron radiation. An accidental predissociation of the $E(0)$, $J=31$ level of e parity was observed by Simmons and Tilford [30]. Baker *et al.* [31] identify the perturber as the $k\ ^3\Pi(v=3)$, $J=31$ level. In their extensive laser spectroscopy study at high temperature, Cacciani *et al.* [12] also observed accidental predissociation for two more J levels ($J_e=41$ and 44), and assigned the perturber as the $k\ ^3\Pi(v=4)$ state.

PREDISSOCIATION YIELD FOR $E\ ^1\Pi(0)$

To determine the predissociation yield of this state, we have used an alternative and entirely different approach that generates complementary information to the uv emission process: direct excitation process. The uv emission gives information after the decay of the excited species takes place, while a direct excitation process determines how the electron-impact excitation occurs. For example, for states with negligible or known cascading and/or branching, the predissociation cross section can be obtained by comparing the measured emission cross section from that state to the corresponding excitation cross section obtained from the electron energy-loss spectrum. The predissociation cross section E state of CO (where the cascade contribution is zero) may be estimated using the following expression:

$$Q_{\rm pre}=Q_{\rm exc}-(Q_{\rm emis}+Q_b), \tag{1}$$

where $Q_{\rm pre}$ is the predissociation cross section, $Q_{\rm exc}$ is the direct excitation cross section, $Q_{\rm emis}$ is the emission cross section of an electronic state (in our case $E\ ^1\Pi$) to the ground state ($X\ ^1\Sigma^+$), and Q_b is the ''branching'' cross section. In Eq. (1), the quantity $Q_{\rm emis}+Q_b$ represents the ''total'' emission cross section. After the initial excitation, the CO molecule can branch down through several intermediate states and produce fluorescence in the wide range of wavelengths, in addition to the direct euv transition to the ground state measured in this work. This approach has been used for the determination of predissociation yields of the c_4', b', and b states of N_2 [19,32] and H_2 Rydberg states [33].

For a negligible or known amount of cascading from an upper state (and/or branching to a lower state), the total emission yield of an excited electronic state i to the ground state x can be defined as

$$(\eta_E)_{i\to x}=\frac{Q_{\rm emis}}{Q_{\rm exc}}. \tag{2}$$

The predissociation yield, η_p, for an excited electronic state of CO may then be estimated using the following expression:

$$\eta_p=1-\left[(\eta_E)_{i\to x}+\sum_k\ (\eta_E)_K\right], \tag{3}$$

where $\Sigma_k(\eta_E)_K$ represents the total emission yield of an excited state to all lower excited electronic states (i.e., branching) other than the ground state. The branching ratio estimates indicate that branching loss from the $E\ ^1\Pi$ state, via $B\ ^1\Sigma^+$, $C\ ^1\Sigma^+$, and $A\ ^1\Pi$ states, accounts for a maximum of only 8% of the total emission observed from the $E\ ^1\Pi$ state [20].

By employing Eqs. (2) and (3), we obtain an 88% predissociation yield for the $E\ ^1\Pi$ electronic state based on the comparison of direct excitation [34] and total emission [15] cross sections and taking into account the 8% emission yield to lower excited states ($B\ ^1\Sigma^+$, $C\ ^1\Sigma^+$, and $A\ ^1\Pi$). Letzelter *et al.* [7] measured predissociation yield for individual vibrational states ($v'=0$ and $v'=1$) of the $E\ ^1\Pi$ electronic state and found 89% and 98% predissociation, respectively. The two measurements for the $E\ ^1\Pi(v'=0)$ state are found to be in excellent agreement.

In the next section, we will present our model of the $E(0,0)$ transition. This model and the data presented in Fig. 5 allows us to obtain predissociation yields for the Π^+ and Π^- sublevels of the $E\ ^1\Pi(0)$ level.

THE CO MODEL

The present measurements of the rotational line intensities of the CO $B(0,0)$, $C(0,0)$, and $E(0,0)$ transitions were modeled by use of Hönl-London factors. The construction of the model for producing synthetic spectra for Σ-Σ and Σ-Π transitions has been described in detail elsewhere [23,33]. Strong perturbations can be neglected, except for weak predissociation of the $E(0)$ vibrational level by an unknown repulsive predissociating state(s). A brief description of the CO model is given below.

The measured intensity I of any rotational line (J',J'') is proportional to the excitation rate. The excitation rate $g(v',J')$ to any upper rotational level J' is given by

$$g(v',J')=Q_{v'}F\sum_{J''=J'-1}^{J''=J'+1}\left[\frac{N(v'',J'')S(J',J'')}{(2J''+1)}\right], \tag{4}$$

where $Q_{v'}$ is the excitation cross section, F is the electron flux, $N(v'',J'')$ is the population in the ground level, and S is the normalized Hönl-London line strength [33]. The rotational line intensities for the $P(J''=J'+1)$ and $R(J''=J'-1)$ branches of the $B(0,0)$ and $C(0,0)$ rovibronic transitions are given by

$$I_{v'v'',J'J''}=g(v',J')\omega_{v'v'',J'J''}, \tag{5}$$

where $\omega_{v'v'',J'J''}$ is the branching ratio, given by

$$\omega_{v'v'',J'J''}=\frac{A_{v'v''}}{A_{v'}}\frac{S(J',J'')}{2J'+1}, \tag{6}$$

where $A_{v'v''}$ is the spontaneous emission transition probability for the (v',v'') band (in our case we limit ourselves to the $v'=v''=0$ case), $A_{v'}$ is the total emission transition probability to all lower vibrational levels v'', given by $A_{v'}=\Sigma_{v''}A_{v'v''}$. We find Eq. (6) is the expression for the case of negligible predissociation.

In order to reproduce, however, the measured spectrum of the $E(0,0)$ band (Fig. 5), the emission branching ratio must have a term that depends on the effects of predissociation. In this case, we write

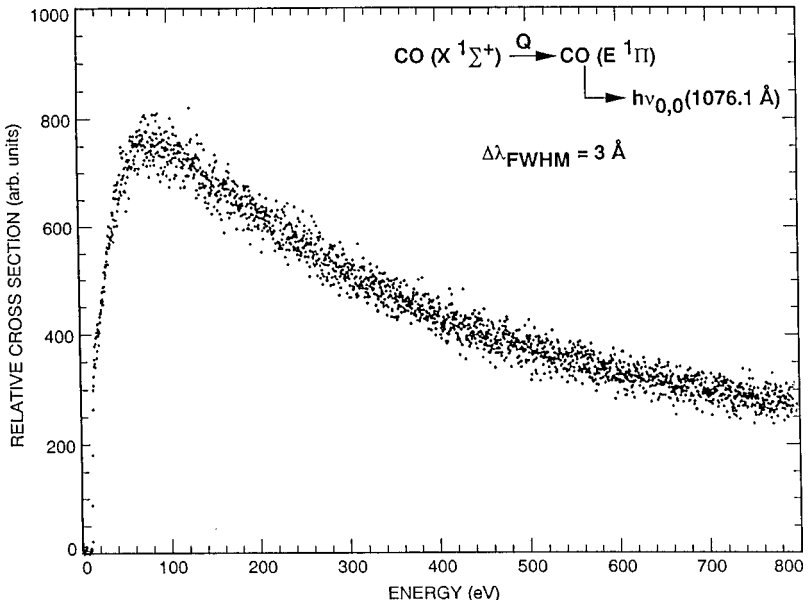

FIG. 6. Relative emission cross section (excitation function) of the CO $E\ ^1\Pi(0,0)$ band (at 1076.1 Å) in the range 0–800-eV electron-impact energy.

$$\omega_{v'v'',J'J''}=\left[\frac{A^+_{v'v''}}{A^+_{v'}}\right]\frac{S(J',J'')}{2J'+1}\,\eta^+_E(v',J'), \tag{7}$$

where $A^+_{v'v''}$ is the spontaneous emission transition probability of the Π^+ (the P and R branches) state, assumed to be constant in J for any v', and analogously for the Π^- state (Q branch) and $\eta^+_E(v',J')$ is an emission yield, given by

$$\eta^+_E(v',J')=\frac{A^+_{v'}}{A^+_{v'}+A^+_{\rm pre}(v',J')}, \tag{8}$$

where $A^+_{v'}+A^+_{\rm pre}(v',J')$ is the total transition probability, and includes the predissociation transition probability $A^+_{\rm pre}(v',J')$ for any $E(0)$ rotational level J'.

The rotational line intensities then become

$$I^+_{v'v'',J'J''}=g(v',J')\,\frac{A^+_{v'v''}S(J',J'')\,\eta^+_E(v',J')}{A^+_{v'}(2J'+1)} \tag{9}$$

and similarly for the Π^- state. The data for the $E(0,0)$ transition, shown in Fig. 5, suggest that $\eta^+_E(J)$ and $\eta^-_E(J)$ are to a good approximation independent of J, although different for the Π^+ and Π^- states, since no sudden weakening of the band is observed, in agreement with observations by Cacciani *et al.* [12]. This yield can then be represented by constants η^+_E and η^-_E. The experiment uniquely determines the ratio between these two yields, since the spontaneous emission probabilities for the Π^+ and Π^- states are independent of J for negligible perturbation with other bound states. It is assumed that the Π^+ and the Π^- emission yields are related to the total emission yield by

$$\frac{\eta^+_E}{2}+\frac{\eta^-_E}{2}=(\eta_E)_{i\to X}. \tag{10}$$

The emission model for the $E\ ^1\Pi(0,0)$ transition, when we assume equal predissociation for the Π^+ and Π^- sublevels, overestimates the brightness of the Q branch. The experimentally determined ratio between the emission yields of the Π^+ and Π^- sublevels is equal to $\eta^-_E/\eta^+_E=0.63$. Using this ratio, and Eq. (10), we obtain $\eta^+_E\approx0.135$ and $\eta^-_E\approx0.085$. From Eq. (3), then, it finally follows that the predissociation yields for the Π^+ and Π^- sublevels (η^+_p and η^-_p, respectively) are $\eta^+_p=0.85$ and $\eta^-_p=0.91$.

Although it is clear from the present measurements that the $E\ ^1\Pi$ state predissociates, the electronic continuum states causing this perturbation are yet to be determined. A list of candidate predissociating states can be found by considering the ways the $C(^3P)$ and $O(^3P)$ atoms can join angular momenta along the internuclear axis. The possible singlet states are $^1\Sigma^+$, $^1\Sigma^-$, $^1\Pi$, and $^1\Delta$ [35,36]. According to the selection rules for predissociation, the E state can be predissociated only by like-parity states. Therefore a repulsive $^1\Sigma^-$ state may be responsible for the enhanced predissociation of the Π^- state observed in this experiment.

OSCILLATOR STRENGTH

Previous experimental and theoretical determinations of oscillator strengths $f_{v'v''}$ from $v''=0$ of the $X\ ^1\Sigma^+$ ground state of CO to different v' levels of the $B\ ^1\Sigma^+$ and $C\ ^1\Sigma^+$ states have been summarized in our earlier paper [15]. In this paper, we report the oscillator strength for the $E\ ^1\Pi(v'=0)\to X\ ^1\Sigma^+(v''=0)$ transition and compare it with other data sets where available.

We obtain the oscillator strength for the $E\ ^1\Pi(v'=0)\to X\ ^1\Sigma^+(v''=0)$ transition by analyzing the energy dependence of the measured excitation function (from 0 to 800 eV) corresponding to that transition. The excitation function for the $E\ ^1\Pi(v'=0)\to X\ ^1\Sigma^+(v''=0)$ transition (Fig. 6) is put on an absolute scale by normalizing

TABLE I. Cross sections at 100 eV for the CO $E\ ^1\Pi(0)$ state (all values in 10^{-18} cm^2).

$Q_{\rm exc}$	=	4.43 ±1.15
$Q_{\rm emis}$	=	0.47 ±0.12
$Q_{\rm pre}$	=	3.91 ±1.02
Q_b	=	0.038±0.01

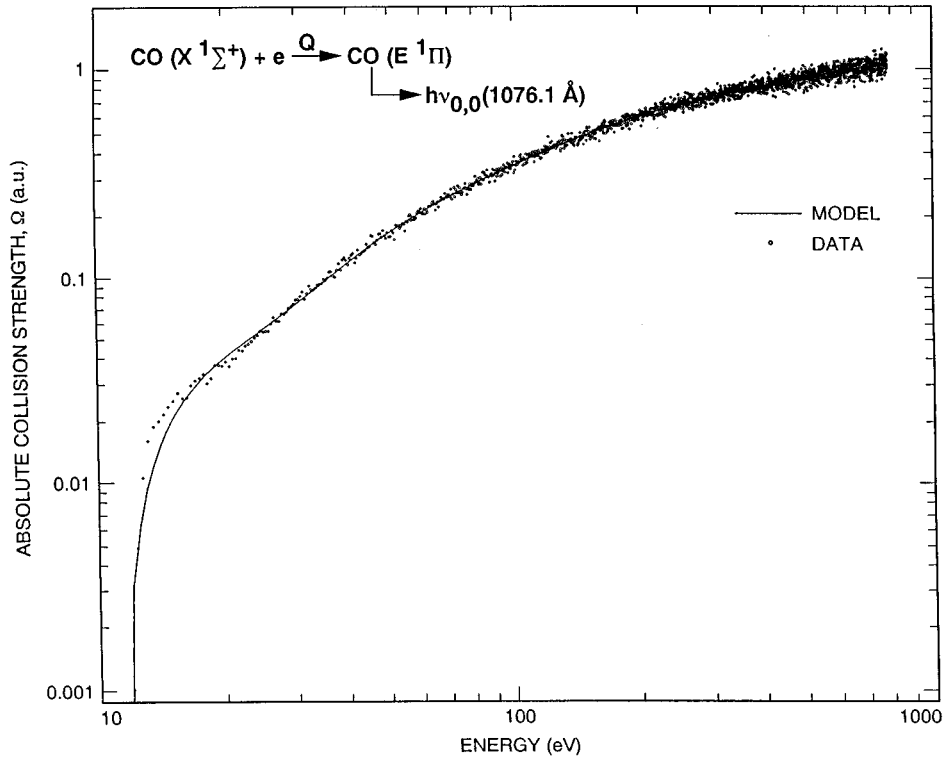

FIG. 7. Model data of the collision strength of the CO $E\ ^1\Pi(0,0)$ band plotted against energy (10–800 eV). The oscillator strength (f value) for this feature is determined as 7.08×10^{-2}.

it to the 100-eV excitation cross sections for the $E\ ^1\Pi(v'=0)\rightarrow X\ ^1\Sigma^+(v''=0)$ transition [34]. From Eq. (1), the predissociation, emission, excitation, and branching cross sections at 100 eV are then obtained, and are reported in Table I. The quoted uncertainty (26%) is due to the error associated with the determination of the excitation cross section [34] and the uncertainties in the fitting procedure, as discussed below.

Collision strength data (cross section times electron impact energy) for the CO $E\ ^1\Pi$ band were fitted within the experimental error (about 20%) using the following analytical form for collision strength:

$$\Omega_{v'v''}(X_{v'v''}) = C_0(1-1/X_{v'v''})(X_{v'v''})^{-2} + \sum_{k=1}^{4} C_k(X_{v'v''}-1)\exp(-kC_8X_{v'v''}) + C_5 + C_6/X_{v'v''} + C_7\ln(X_{v'v''}), \quad (11)$$

where $\Omega_{v'v''}(X_{v'v''})$ is the collision strength, $X_{v'v''}$ is the electron-impact energy in threshold units, and C_k are constants of the function $\Omega_{v'v''}(X_{v'v''})$ [21,22]. The result of this fit is reported in Fig. 7. The constant C_0 represents the contribution of electron exchange, C_1-C_4 represent configuration mixing, C_5-C_6 represent polarization effects, C_7 is the Born term, and C_8 is a constant in the mixing terms. Table II gives the constants of Eq. (11) for the CO $E\ ^1\Pi(v'=0)\rightarrow X\ ^1\Sigma^+(v''=0)$ transition. The excitation cross section is given by the equation

$$\sigma_{v'v''}(X_{v'v''}) = \Omega_{v'v''}(X_{v'v''})(E_{v'v''}X_{v'v''})^{-1}, \quad (12)$$

where $\sigma_{v'v''}(X_{v'v''})$ is the cross section in atomic units, and $E_{v'v''}$ is the transition energy in Rydberg units. At the high-energy limit the collision strength has the following form:

$$\Omega_{v'v''}(X_{v'v''}) \approx C_5 + C_7\ln(X_{v'v''}), \quad X_{v'v''} \gg 1. \quad (13)$$

In the Bethe approximation [37], the collision strength is given by

$$\Omega_{v'v''}(X_{v'v''}) = \omega_{v''}\left(\frac{8ma_0^2}{\hbar^2}\right)\frac{f_{v'v''}}{E_{v'v''}} \times(\ln X_{v'v''} + 4C_{v'v''}E_{v'v''}), \quad (14)$$

where $\omega_{v''}$ is the lower state degeneracy, $C_{v'v''}$ is a constant, related to the angular distribution of the scattered electrons, $f_{v'v''}$ is the oscillator strength, a_0 is the Bohr radius, m is electron mass, and $\hbar$ is the Planck's constant. Thus

$$C_7 = \omega_{v''}\left(\frac{8ma_0^2}{\hbar^2}\right)\frac{f_{v'v''}}{E_{v'v''}}. \quad (15)$$

TABLE II. Constants of the modified born equation $\Omega_{v'v''}(X_{v'v''}) = C_0(1-1/X_{v'v''})(X_{v'v''})^{-2} + \Sigma_{k=1}^{4}C_k(X_{v'v''}-1) \times\exp(-kC_8X_{v'v''})+C_5+C_6/X_{v'v''}+C_7\ln(X_{v'v''})$.

Constant	$E\ ^1\Pi$
C_0	0
C_1	−0.11229
C_2	0.58790
C_3	−1.7784
C_4	1.8675
C_5	−0.35586
C_6	0.35586
C_7	0.33437
C_8	0.26915

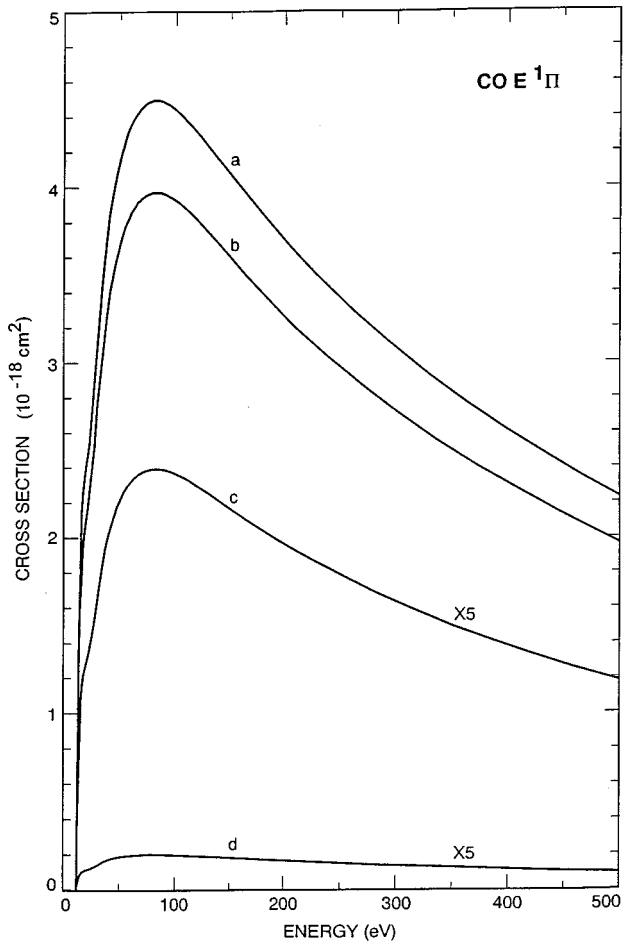

FIG. 8. Model fit for the excitation (curve *a*), predissociation (curve *b*), emission (curve *c*), and branching (curve *d*) cross sections for the CO $E\ ^1\Pi(0)$ state. Emission and branching cross sections are multiplied by a factor of 5.

As seen in Eq. (15), the optical oscillator strength can be related to one of the constants in the fitting function at the high-energy limit. This equation allows us to determine the oscillator strength. For the CO $E\ ^1\Pi(0)\rightarrow X\ ^1\Sigma^+(0)$ transition the optical oscillator strength was found to be 7.08×10^{-2}. The experimental collision strength and the analytic fitting function for the CO $E\ ^1\Pi(0)\rightarrow X\ ^1\Sigma^+(0)$ transition are shown in Fig. 7. The error associated with the oscillator strength is estimated as follows: (a) 26% error from the CO $X\rightarrow E$ excitation cross section [34] and (b) 5% error estimated from the fitting procedure (based on the goodness of the fit). Thus the overall error (square root of the sum of the squares of the contributing errors) in the oscillator strength is estimated to be about 26%. In our previous work [15] low-energy secondary electrons in the electron beam could contribute up to 10% error to the measured oscillator strength. A redesigning of the electron gun and the Faraday cup, with a new set of apertures that follow the divergence of the *e* beam and a lower magnetic field, prevents trapping of the secondary electrons in the interaction region and therefore substantially reduces their influence on the measurements in the high-energy range. Thus, the determination of the oscillator strength, which relies on the collision strength fit in the high energy, is not affected by the secondary electrons.

TABLE III. Summary of previous and present determinations of oscillator strength $f_{v'v''}$ for the transition between the CO $E\ ^1\Pi(0)$ state and the ground state $X\ ^1\Sigma^+(0)$.

Source	f_{00} (units, of 10^{-2})
Kirby and Cooper (theory) [2]	4.9
Stark *et al.* [9]	4.9 $\pm$0.5
Eidelsberg *et al.* [6][a]	3.65$\pm$0.37
Lee and Guest [17]	1.81$\pm$0.27
Chan *et al.* [38]	7.06$\pm$0.7
Lassetre and Skerbele [39]	9.40$\pm$0.85
This work	7.08$\pm$1.8

[a]From absorption experiment data of Letzelter *et al.* [7]

Since there is no cascading into the $E(0)$ state, we can assume that the energy variation of the excitation, predissociation, emission, and branching cross sections is the same. From the analytical fit of the excitation function and by using Eq. (1), we then obtain analytical fits to the predissociation and branching (as stated earlier, branching to lower excited states is 8% of the total emission) cross sections, shown in Fig. 8, in the 0–500-eV range. Also shown are excitation and emission cross sections.

There are many reported experimental and theoretical data for the oscillator strength of the $E\ ^1\Pi$ state. Table III summarizes the oscillator strength values obtained by different researchers for the CO $E\ ^1\Pi(0)\rightarrow X\ ^1\Sigma^+(0)$ transition, with their quoted uncertainties. Large variations exist among these values. A comparison of the oscillator strengths gives an excellent agreement between the present result and that of Chan *et al.* [38] (disagreement is less than 1%) and well within the respective error limits. There is also fair agreement between the data of Lassettre and Skerbele [39] and the present value. In fact, while our measurement is about 33% lower than that of Ref. [39], they agree within the combined error limits. The theoretical result of Kirby and Cooper [2] is about 31% lower than the present result and agrees with the result of Stark *et al.* [9], while the value of Lee and Guest [17] is 3.9 times smaller than ours, much beyond their quoted uncertainty of 15%. Our value is also about 1.9 times larger than the value obtained by Eidelsberg *et al.* [6] from Letzelter *et al.* [7] data. However, the $E\ ^1\Pi$ band is subject to pressure saturation effect. Therefore, the values of the oscillator strengths reported by Ref. [17] and Refs. [6, 7] for the $E\ ^1\Pi\rightarrow X\ ^1\Sigma^+$ transition may well be affected by pressure saturation effects.

The values of the oscillator strength found here may have important implication for models of CO photodestruction in the ISM. Letzelter *et al.* [7] have measured the set of absorption cross section used for modeling CO absorption at photon energies below the Lyman continuum threshold. The data of Letzelter *et al.* [7] for the singlet-state Rydberg series are used as a benchmark for CO photodestruction [1]. A factor of 2 increase in photodissociation yield of the largest single contributor to predissociation for this molecular state needs to be considered in future ISM modeling.

ACKNOWLEDGMENTS

The research described in this paper was carried out at the Jet Propulsion Laboratory, California Institute of Technol-

ogy, and was sponsored by the U.S. Air Force Office of Scientific Research (AFOSR), the Aeronomy Program of the National Science Foundation (ATM-9320589), and National Aeronautics and Space Administration (Planetary Atmospheres, Astronomy/Astrophysics, and Space Physics Program Offices). One of us (M.C.) is supported by the National Research Council. The authors also wish to thank W. Ubachs and F. Rostas for valuable discussions and suggestions, and J. Kendall for a careful reading of the manuscript.

[1] E. F. van Dishoeck and J. H. Black, Astrophys. J. **334**, 771 (1988).
[2] K. Kirby and D. L. Cooper, J. Chem. Phys. **90**, 4895 (1989).
[3] Y. P. Viala, C. Letzelter, M. Eidelsberg, and F. Rostas, Astron. Astrophys. **193**, 265 (1988).
[4] E. F. van Dishoeck and J. H. Black, in *Physical Processes in Interstellar Clouds*, edited by G. E. Morfill and M. Scholer (Reidel, New York, 1987), p. 241.
[5] M. Eidelsberg and F. Rostas, Astron. Astrophys. **235**, 472 (1990).
[6] M. Eidelsberg, J. J. Benayoun, Y. Viala, and F. Rostas, Astron. Astrophys. Suppl. **90**, 231 (1991).
[7] C. Letzelter, M. Eidelsberg, F. Rostas, J. Breton, and B. Thieblemont, Chem. Phys. **114**, 273 (1987).
[8] G. Stark, K. Yoshino, P. L. Smith, K. Ito, and W. H. Parkinson, Astrophys. J. **369**, 574 (1991).
[9] G. Stark, P. L. Smith, K. Ito, and K. Yoshino, Astrophys. J. **395**, 705 (1992).
[10] G. Stark, K. Yoshino, P. L. Smith, J. R. Esmond, K. Ito, and M. Stevens, Astrophys. J. **410**, 837 (1993).
[11] M. Drabbels, J. Heinze, J. J. ter Meulen, and W. L. Meerts, J. Chem. Phys. **99**, 5701 (1993).
[12] P. Cacciani, W. Hogervorst, and W. Ubachs, J. Chem. Phys. **102**, 8308 (1995).
[13] W. Ubachs, P. C. Hinnen, P. Hansen, W. Hogervorst, and P. Cacciani, J. Mol. Spectrosc. **174**, 388 (1995).
[14] D. C. Norton and L. Noreau, Astrophys. J. Suppl. **95**, 301 (1994).
[15] I. Kanik, G. K. James, and J. M. Ajello, Phys. Rev. A **51**, 2067 (1995).
[16] E. F. van Dishoeck, in *Astrochemistry*, edited by M. S. Vardya and S. P. Tarafdar (Reidel, Dordrecht, 1987), p. 51.
[17] L. C. Lee and J. A. Guest, J. Phys. B **14**, 3415 (1981).
[18] W. Ubachs, K. S. E. Eikema, P. F. Levelt, W. Hogervorst, M. Drabbels, W. L. Meerts, and J. J. Ter Meulen, Astrophys. J. **427**, L55, 1994.
[19] J. Ajello, G. K. James, and B. O. Franklin, Phys. Rev. A **40**, 3524 (1989).
[20] G. K. James, J. M. Ajello, I. Kanik, B. O. Franklin, and D. Shemansky, J. Phys. B **25**, 1481 (1992).
[21] D. E. Shemansky, J. M. Ajello, and D. T. Hall, Astrophys. J. **296**, 765 (1985).
[22] D. E. Shemansky, J. M. Ajello, D. T. Hall, and B. O. Franklin, Astrophys. J. **296**, 774 (1985).
[23] X. Liu, S. M. Ahmed, R. Multari, G. K. James, and J. M. Ajello, Astrophys. J. Suppl. **101**, 375 (1995).
[24] S. G. Tilford and J. T. Vanderslice, J. Mol. Spectrosc. **26**, 419 (1968).
[25] R. J. Kelly, *Atomic and Ionic Spectrum Lines below 2000 Angstroms: Hydrogen through Krypton*, special issue of J. Chem. Ref. Data, **16**, Suppl. 1 (1987).
[26] M. Eidelsberg, J.-Y. Roncin, A. LeFloch, F. Launay, C. Letzelter, and J. Rostas, J. Mol. Spectrosc. **121**, 309 (1987).
[27] K. P. Huber and G. Herzberg, *Molecular Spectra and Molecular Structure: IV. Constants of Diatomic Molecules* (Van Nostrand, New York, 1979).
[28] J. J. Hopfield and R. T. Birge, Phys. Rev. **29**, 922 (1927).
[29] S. G. Tilford, J. T. Vanderslice, and P. G. Wilkinson, Can. J. Phys. **23**, 450 (1965).
[30] J. D. Simmons and S. G. Tilford, J. Mol. Spectrosc. **49**, 167 (1974).
[31] J. Baker, J. L. Lemaire, S. Couris, A. Vient, D. Malmasson, and F. Rostas, Chem. Phys. **178**, 569 (1993).
[32] G. K. James, J. M. Ajello, I. Kanik, B. O. Franklin, and D. Shemansky, J. Phys. B **23**, 2055 (1990).
[33] J. M. Ajello, D. Shemansky, T. L. Kwok, and Y. L. Yung, Phys. Rev. A **29**, 636 (1984).
[34] I. Kanik, M. Ratliff, and S. Trajmar, Chem. Phys. Lett. **208**, 341 (1993).
[35] D. E. Shemansky, I. Kanik, and J. M. Ajello, Astrophys. J. **452**, 480 (1995).
[36] G. Herzberg, *Molecular Spectra and Molecular Structure: I. Spectra of Diatomic Molecules* (Krieger Publishing, Malabar, FL, 1989).
[37] H. A. Bethe, Ann. Phys. (N.Y.) **5**, 325 (1930).
[38] W. F. Chan, G. Cooper, and C. E. Brion, Chem. Phys. **170**, 123 (1993).
[39] E. N. Lassettre and A. Skerbele, J. Chem. Phys. **54**, 1597 (1971).